Scanning Tunneling Microscopy, Fourier Transform Infrared Reflection−Absorption Spectroscopy, and X-ray Photoelectron Spectroscopy of Thiourea Adsorption from Aqueous Solutions on Silver (111)

V. Brunetti, B. Blum, R. C. Salvarezza, and A. J. Arvia*

Instituto de Investigaciones Físicoquímicas Teóricas y Aplicadas (INIFTA), Universidad Nacional de La Plata-CONICET, Sucursal 4, Casilla de Correo 16, (1900) La Plata, Argentina

P. L. Schilardi† and A. Cuesta

Instituto de Química Física Rocasolano, C.S.I.C., C. Serrano, 119, E-28006 Madrid, España

J. E. Gayone and G. Zampieri

Centro Atómico Bariloche and Instituto Balseiro, Comisión Nacional de Energía Atómica and Universidad Nacional de Cuyo, Av. Bustillo 9500, (8400) Bariloche, Argentina

Received: April 12, 2002; In Final Form: May 31, 2002

Thiourea (TU) adsorption on Ag(111) from aqueous solutions was investigated by in situ scanning tunneling microscopy operating under potential control. Hexagonal arrangements with $d = 0.44$, 0.38, and 0.33 nm were imaged at potentials close to −1.2 V (vs SCE), where conjugated voltammetric current peaks are observed. The analysis of in situ Fourier transform infrared reflection−absorption spectra (FT-IRRAS) shows that these current peaks mainly involve electroadsorption/electrodesorption of TU on the Ag(111) surface. Data from ex situ X-ray photolectron spectroscopy of TU-covered Ag(111) closely resemble those obtained for adsorbed alkanethiols on the same substrate, suggesting that the canonical form of TU is the species adsorbed from aqueous solutions. Experimental evidence of TU degradation into other sulfur species is also observed.

1. Introduction

The understanding of adsorbate/substrate, adsorbate/adsorbate, and adsorbed−adsorbable molecule/solvent interactions is a crucial point in the development of ultrathin 2D structures with potential applications for nanofabrication, corrosion protection, and electroanalysis. Adsorption of S-containing and N-containing molecules on Au(111) and Ag(111) has been taken as model systems to gain information on the role of the different interactions in the self-assembly processes. In recent years, most of the experimental and theoretical work in this area has been concentrated on S and alkanethiols (HSR, R = C_nH_{2n+1}) on metals,[1] in particular on Au(111) and to a lesser extent on Ag(111). Alkanethiols bond strongly to these metals by the S-head, upon adsorption.[2] In aqueous media, it is now well-established that both intermolecular forces and hydrophobicity of the molecules play key roles in the electroadsorption/electrodesorption behavior of alkanethiols on Au(111) and Ag(111). In fact, hydrocarbon chain/chain and chain/water interactions influence the electrodesorption potential of these self-assembled molecular arrays, both depending on the chain length.[1]

Thiourea (TU) (Table 1) is an interesting short S- and N-containing molecule. TU and substituted TU have been widely used as additives in plating baths to prepare bright and smooth electrodeposited metal surfaces[3−4] and to hinder corrosion processes by forming adsorbed organic layers.[2] The electroadsorptive response of TU on Au(111) is similar to that of other S-bonded molecules;[5] in contrast, for instance, tetra methyl thiourea (TMTU) (Table 1) presents adsorptive behavior involving both S and N.[6]

TABLE 1: Chemical Formulas for Thiourea and Related Compounds

Molecule	Formula
TU (normal)	$S{=}C\langle^{NH_2}_{NH_2}$
TMTU	$S{=}C\langle^{NM_2}_{NM_2}$
TU (canonical)	$H{-}S{-}C\langle^{NH}_{NH_2}$
FDS	$^{NH}_{NH_2}\rangle C{-}S{-}S{-}C\langle^{NH}_{NH_2}$

M = CH_3

At first sight, it would seem incongruous to compare TU adsorption on metals with sulfide or thiolate adsorption. However, in the thiocarbonyl bond, such as in TU, the overlapping of the C $2p_\pi$ orbital with the S $3p_\pi$ orbital is not very favorable and renders the C═S bond unstable.[7] Thiocarbonyl bonds are therefore unstable. They stabilize by conjugate electron displacements. The sulfur headgroup of the canonical form of TU (Table 1)[8] is functionally similar to thiol-S headgroups, and this canonical form is the TU species found to adsorb on Ag(111) and Cu(111),[8] presumably with a cleaved S−H bond, which occurs with S-containing molecules below 200 K,[9] and in particular for thiol adsorption on gold and silver.[10]

* Corresponding author. E-mail: ajarvia@inifta.unlp.edu.ar.
† Permanent address: INIFTA-UNLP-CONICET, Sucursal 4, CC 16, (1900) La Plata, Argentina.

10.1021/jp0209695 CCC: $22.00 © 2002 American Chemical Society
Published on Web 08/31/2002

The S−C bond in sulfur-containing molecules usually cleaves at temperatures between 250 and 400 K.[9] During dissociation of organosulfur molecules on metals, sulfur and carbon atoms are left on the surface, whereas hydrogen molecules and hydrocarbon species desorb into the gas phase.[9] As an example, sulfur and alkanethiols at room temperature form very stable monolayers on gold. Prolonged (37 h) exposure to thiols[11] and other sulfur-containing compounds[12] in the presence of water produces extensive sulfidation of silver surfaces in the form of a thin interfacial layer of Ag_2S, as determined by X-ray photoelectron spectroscopy (XPS)[11,12] and related techniques.[12] Alkanethiol adsorption reactions on copper and nickel often involve several coadsorbed molecular moieties.[13,14] TU adsorption on metals is even more complex because of its high chemical reactivity both in the aqueous electrolyte solution and in the adsorbed state. In fact, little agreement has been obtained as to whether TU reacts in the aqueous solution or at the metal surface, yielding either different sulfur-containing organic species or elemental sulfur or both simultaneously. In turn, intermediate products can be adsorbed on the surface for further reactions. Therefore, the chemistry specifically depends on both the metal and the organosulfur molecule.

Voltammetric electrodesorption of sulfur and sulfur-containing molecules from Ag(111)[15−21] and Au(111)[5,22] results in similar current peak multiplicities under comparable experimental conditions, even though electrochemical waves for silver are systematically shifted negatively by approximately 0.3 eV as a result of the work function differences between both materials.[22] There is much disparity in the literature as to whether the different voltammetric peaks are the result of different sulfur−adsorbate structure formation on the Ag(111)[15] terraces, ionic adsorption after organosulfur desorption,[16,17,23] thiol adsorption on different Ag(111) [21] or Au(111)[24] sites, or coverage-dependent interactions between adjacent hydrocarbon chains.[20] Whereas in the particular cases of sulfur[25,26] and alkanethiol[24,27,28] adsorption on Au(111) it now seems clear that the different voltammetric peaks are associated with sulfur species adsorbed on terrace or step-edge sites, for TU adsorption on Au(111),[5] they are associated with different sulfur-containing species.

Sulfur and sulfur-containing molecule adsorption on Ag(111)[15,29−34] and Au(111)[1,35] result in ordered hexagonal arrays with typical $d = 0.44-0.46$-nm and $d = 0.50$-nm intermolecular spacings, respectively. The different intermolecular spacings, on either substrate, result from a detailed balance of adsorbate−substrate and hydrocarbon chain−chain interactions.[1] For the latter, the strongly site-dependent sulfur−gold interaction precludes the formation of the more compact $d = 0.44$-nm phase allowed by van der Waals hydrocarbon chain repulsions, except in the case of TU adsorption on Au(111), where the even stronger adsorbate/adsorbate interaction overcomes this barrier, forming compact $d = 0.33$-nm phases.[5]

Recent in situ scanning tunneling microscopy (STM) data show that thiourea adsorption on Au(111) is sequentially followed by its oxidation to formamidine disulfide (FDS) (Table 1), which, depending on the applied potential and immersion time, in turn transforms into either sulfur mono- or multilayers.[5] There is no equivalent study, to our knowledge, on Ag(111). Given the different structures formed upon adsorption of TU on Au(111)[5] and Ag(111)[18] and the different reactivities of organosulfur molecules upon adsorption on gold and silver, the formation of differently ordered TU structures on Ag(111) cannot be directly inferred from electroadsorption results on Au(111).

In the present work, room-temperature TU adsorption on Ag(111) from aqueous solutions examined with in situ STM under potential control reveals the presence of hexagonal arrangements with $d = 0.44$, 0.38, and 0.33 nm (section 3.2) at potentials close to the voltammetric peaks located at $E = -1.2$ V (vs SCE) (section 3.1). To gain a better insight into the chemical identity of the adsorbed species, TU adsorption on polycrystalline Ag electrodes was also investigated with in situ Fourier transform infrared reflection−absorption spectroscopy (FT-IRRAS) in the same potential regions. These analyses show that the voltammetric peaks at $E = -1.2$ V mainly involve electroadsorption/electrodesorption of TU on the Ag(111) surface. (section 3.3) Ex situ X-ray photoelectron spectra of TU-covered Ag(111) closely resemble those obtained for adsorbed alkanethiols on the same substrate, suggesting that the canonical form of TU is the species adsorbed from solution (section 3.4).

2. Experimental Section

2.1. Sample Preparation. A high-purity (99.999%) cylindrical silver single crystal, 2 mm thick and 10 mm in diameter, was oriented and cut parallel to the (111) plane (miscut <2°). The surface was then mechanically polished down to 0.05 μm with alumina and annealed for 45 min at 823 K in a hydrogen furnace. Before each experiment, the electrode was etched for a few seconds with 1:1 (V/V) mixture of 40% hydrogen peroxide and 30% ammonia to remove the outermost, distorted/contaminated lattice layers and was rinsed thoroughly with water. Typical Ag(111) surfaces are formed by large (∼130 nm) terraces limited by step bunches and narrow (<2 nm) terraces.[18]

2.2. Voltammetry. Voltammetric runs with Ag(111) working electrodes were carried out at 300 K in a conventional glass cell with a platinum counterelectrode and a saturated calomel reference electrode (SCE) utilizing a PAR 373 potentiostat. High-purity chemicals and Milli-Q water were used to prepare deaerated aqueous 50 μM TU + 0.1 M NaOH. Fresh solutions were used in all cases because of the high reactivity of TU in aqueous solutions. Several potential time routines were used, changing the holding time and the values of the anodic (E_a) and cathodic (E_c) switching potentials. These routines are specified in each voltammogram.

2.3. Scanning Tunneling Microscopy. In situ STM images were taken at 298 K with a Digital Instruments Inc. Nanoscope III electrochemical STM setup. Commercial (Digital Instruments, Santa Barbara, CA) and scissors-snipped 90% Pt−10% Ir tips were used in air and were coated with Apiezon wax for electrochemical observations.

The STM electrochemical cell was made of Kel-F and consisted of a Ag(111) single crystal as a working electrode, a large-area platinum counterelectrode, and a palladium/hydrogen reference electrode, although all values of potential (E) in the text are given on the SCE scale. Samples were first immersed at open circuit potential (*ocp*) in aqueous 50 μM TU + 0.1 M NaOH. The potential was then swept downward to the hydrogen evolution reaction (*her*) and finally stepped upward of the first TU electroadsorption peak, where the samples were imaged. Imaging potentials are indicated in the respective figure captions.

Images were plane-removed and flattened using commercial image-processing software to correct for tilt and bow.

2.4. Fourier Transform Infrared Reflection−Absorption Spectroscopy (FT-IRRAS). In situ FT-IRRAS measurements were carried out in a three-electrode electrochemical cell with a fluorite 60° prism attached to it, using a platinum wire as the

counterelectrode, a polycrystalline silver disk (diameter 1.2 mm) as the working electrode, and a SCE reference electrode. The cell was placed in a Perkin-Elmer 1725X FT-IRRAS spectrometer, and the potentials were applied through an EG&G PAR 362 potentiostat. The polycrystalline disk was chosen on the basis of the geometry of the FT-IRRAS cell that was available and on the similarity in voltammetric responses of polycrystalline silver and Ag(111) under comparable conditions. Prior to each run, the working electrode was polished to mirror grade with 0.05 μm alumina and then was sonicated and rinsed with distilled water. The electrolyte solution, 50 μM TU + 0.05 M sodium perchlorate, was prepared from analytical reagent-grade chemicals and D_2O and bubbled with nitrogen both 2 h prior to and during each run.

Each measurement involved the application of a sequence of potential steps $\Delta E = -0.1$ V, from $E_i = -0.6$ V to $E_f = -1.2$ V, taking as reference the spectrum obtained at $E_R = -0.2$ V. At each potential, 100 interferometer scans were taken, implying a step time of about 40 s.

2.5. X-ray Photoelectron Spectroscopy. XPS spectra of a Ag(111) sample dipped for 10 s in aqueous 50 μM TU at the *ocp* were acquired with Al Kα radiation ($h\nu = 1486.6$ eV) using a hemispherical energy analyzer. Both survey and S 2p-specific spectra were acquired. Binding energies (BE) were referenced to the Ag $3d_{5/2}$ BE, which was set at 367.9 eV.[36] This BE assignment is reasonable, taking into account the <0.1 eV shifts observed in Ag(I) peak positions by organosulfur molecule adsorption.[37,38] The error in the S 2p BE peak positions is estimated to be $\pm$0.3 eV.

Given the very small signal-to-noise ratio encountered, 6 separate, cumulative S 2p photoelectron spectra of this sample were acquired, totaling more than 2000 scans. The S 2p spectra were fit with a variable number of spin−orbit-split S $2p_{1/2,3/2}$ doublets represented by two Gaussian functions separated by 1.15 eV[39] with a 1:2 intensity ratio.[36]

Possible sample degradation as a result of X-ray radiation or deteriorated vacuum conditions during the prolonged (>30 h) spectra acquisition period was checked by comparing early and late spectra.

3. Interpretation and Discussion of Results

3.1. Electrochemical Response. Typical cyclic voltammograms of Ag(111) in aqueous 50 μM TU + 0.1 M NaOH recorded at 0.250 V s^{-1} between $E_c = -1.5$ V and $E_a = -0.4$ V after first waiting 5 min at E_c (Figure 1a) show a broad anodic current peak at $E = -1.17$ V (AII) and a better-defined cathodic current peak at $E = -1.23$ V (CII). These peaks, in principle, can be related to TU adsorption/desorption, respectively. At $E > -0.7$ V, a slight increase in anodic current (AI) is observed. If the reverse scan is extended to potentials more negative than $E = -1.5$ V, the *her* takes place.

Assuming a single electron-transfer process and subtracting the charge density involved in the *her*, the charge density of peak CII results in $q_c = 116$ μC cm^{-2}, a value that corresponds to a degree of surface coverage (θ) in monolayer units (ML) of $\theta = 0.52$ ML (1 ML Ag(111) = 1.388×10^{15} atoms cm^{-2}).

Cyclic voltammograms of polycrystalline Ag in aqueous 50 μM TU + 0.05 M sodium perchlorate are practically the same as those shown in Figure 1, with the peak pair AII/CII potential shifted slightly (0.09 V) in the positive direction. Overall, a slight shift (<0.1 V) of peak potentials in the negative direction is observed as the pH is changed from 6 to 13 (0.1 M NaOH) as a result of protonation/deprotonation of the molecular species adsorbed/desorbed at the pair of peaks AII/CII. The overall

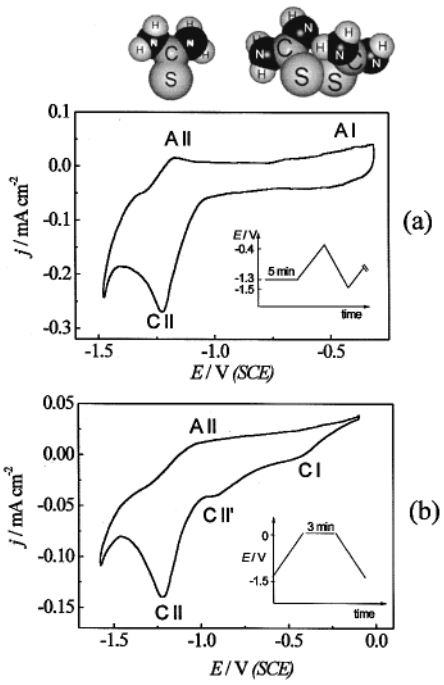

Figure 1. Voltammograms of Ag(111) in aqueous 50 μM TU + 0.1 M NaOH run at 0.25 V sec^{-1}, 300 K. (a) Steady-state cyclic voltammogram including space-filling models of associated TU and FDS molecules. (b) Voltammogram resulting after holding the potential at $E = 0$ V for 3 min. Insets: applied potential routines.

electrochemical response of the TU/Ag(111) system is also similar to that of the TU/Au(111) system,[5] although the shift of ~0.3 V in the positive direction of the potential window where the latter's reactions take place is a direct consequence of the differences in substrate work functions.

Alternatively, when E is held at potentials positive to that of peak AII, the voltammogram shows the presence of new peaks in region II, which are also found in the electrochemical response of silver in sulfide solutions.[15] In particular, when the potential is held for 3 min at $E = 0$ V (Figure 1b), two cathodic current peaks CII and CII′ in region II and a cathodic peak CI are observed. As occurs on Au(111),[5] the electroreduction of sulfur species such as FDS and sulfur to produce TU could be the origin of peak CI. Peak CII, which is discussed together with the STM data below, is observed, irrespective of the E holding value, positive to that of peak AII in all experiments performed. Electrodesorption voltammograms in 0.1 M NaOH of Ag(111) previously dipped in aqueous 50 μM TU[18] always show peak CII and reveals the same peak multiplicity with sufficient dipping time (20 s) at *ocp*[18] as that shown in Figure 1. Note that during dipping the potential is positive to that of peak AII.

3.2. In Situ STM Imaging. The main ordered structures observed by in situ STM at potentials positive with respect to the anodic current peak AII are summarized in Figures 2 and 3. The images depicted in Figure 2, obtained at $E = -1.275$ V, show the typical hexagonal structure with a nearest-neighbor distance of $d = 0.44 \pm 0.02$ ($\theta = 0.43$) corresponding to a Ag(111)−($\sqrt{7} \times \sqrt{7}$)R 19.1°−3X structure (Figure 2c). This generic structure has been reported for the adsorption of both sulfur and short alkanethiols on the same substrate;[29,31] therefore, X could correspond to either TU or sulfur, considering the high reactivity of TU both in solution and adsorbed on metallic surfaces.[3] In the $-1.19 < E/V < -0.65$ potential region, a slightly more condensed Ag(111)−($\sqrt{7} \times \sqrt{7}$)R 19.1°−4X hexagonal structure with $d = 0.38 \pm 0.02$ nm and $\theta = 0.57$ (Figure 3) was observed. While the $d = 0.38$-nm hexagonal

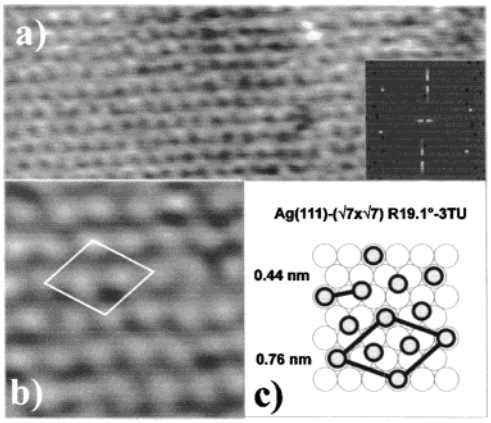

Figure 2. In situ STM top-view images of Ag(111) in aqueous 50 μm TU + 0.1 M NaOH at $E = -1.275$ V, $E_{bias} = 580$ mV, $I_t = 7.6$ nA. (a) 11 × 4 nm^2. Inset: Fourier transform. (b) 2.5 × 2.5 nm^2. (c) Scheme of the Ag(111)−($\sqrt{7} \times \sqrt{7}$)*R* 19.1°−3TU adsorbate structure. Characteristic intermolecular distances are indicated.

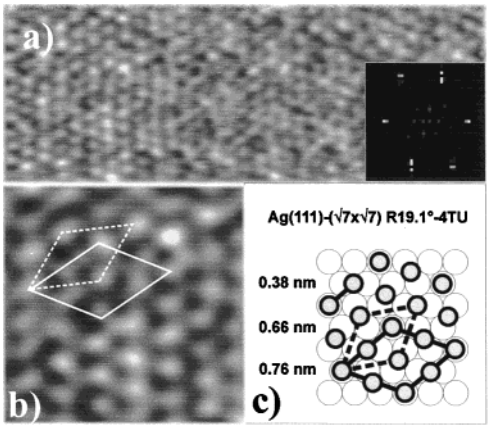

Figure 3. In situ STM top-view images of Ag(111) in aqueous 50 μm TU + 0.1 M NaOH at $E = -1.185$ V, $E_{bias} = 402$ mV, $I_t = 17.6$ nA. (a) 11 × 4 nm^2. Inset: Fourier transform. (b) 2.5 × 2.5 nm^2. (c) Scheme of the Ag(111)−($\sqrt{7} \times \sqrt{7}$)*R* 19.1°−4TU adsorbate structure. Characteristic intermolecular distances are indicated.

structure has not previously been reported for sulfur or alkanethiolate adsorption on Ag(111), $d = 0.38$ nm is one of the three characteristic sulfur trimer distances found upon sulfide adsorption on this substrate.[15,40] This regular hexagonal $d = 0.38$-nm structure does, however, appear to be novel, and as such, it is tempting to assign X to TU. These two open hexagonal lattices involving hollow and top adsorption sites are consistent with those reported for other S-containing molecules on Ag(111) and result from the small energy differences between the different adsorption sites of the Ag(111) face.

In addition to these two hexagonal lattices, domains with structures as compact as hexagonal $d = 0.33 \pm 0.02$ nm ($\theta = 0.75$) are observed (Figure 4). This hexagonal close-packed structure has also been reported for TU adsorption on Au(111).[5] In this case, the adsorbate−adsorbate interaction is strong enough to overcome the pronounced site-dependent adsorbate-site interaction on the Au(111) surface and form a condensed $d = 0.33$-nm ordered structure.

Combined electrochemical and STM imaging results suggest that the surface coverage of the Ag(111) substrate by TU is a slow process of several minutes that takes place at different rates so that different surface structures coexist spatiotemporally. The intermediate value of $\theta = 0.52$ determined from the corresponding q_c value supports this interpretation. Therefore, the multiple voltammetric peaks (CII, CII′) observed in potential region II could possibly be associated with a slow transformation between the three different adsorbate-induced hexagonal surface structures and multilayer formation.

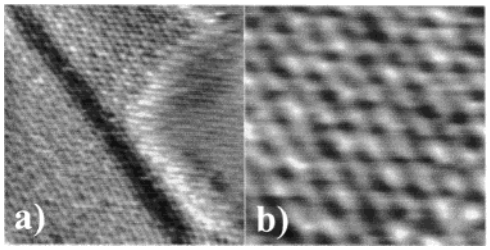

Figure 4. Hexagonal close-packed $d = 0.33$-nm in situ STM top-view images of Ag(111) in aqueous 50 μm TU + 0.10 M NaOH at $E = -1.185$ V, $E_{bias} = 402$ mV, $I_t = 17.6$ nA. (a) 10 × 10 nm^2 showing two domains at both sides of the step. (b) 2.5 × 2.5 nm^2.

However, given the complexity of TU adsorption reactions in aqueous electrolytes,[41,42] we cannot definitely assert at this stage whether the Ag(111)−($\sqrt{7} \times \sqrt{7}$)*R* 19.1°−4X and Ag(111)−($\sqrt{7} \times \sqrt{7}$)*R* 19.1°−3X structures are formed as a result of sulfur or TU adsorption. In fact, cyclic voltammograms in aqueous 50 μM Na_2S of Ag(111) resulted in a single pair of peaks and values of q_c comparable to those described in Figure 1. Thus, the assignment of these surface structures to either sulfur or TU, solely from in situ STM and electrochemical data, is inconclusive.

3.3. FT-IRRAS Data. In situ FT-IRRAS experiments of polycrystalline silver were performed in 50 μM TU + 0.05 M $NaClO_4$ solution. In this solution, the voltammetric features (Figure 5a) of the pair of peaks AII/CII are practically the same as those shown in Figure 1a.

To identify the nature of the main adsorbates on silver at different *E* values, s- and p-polarized light was used. Given that the electrochemical double layer is approximately 1 nm (i.e., $\nu/10000$, where $\nu = 1/\lambda$, is the wavenumber), the s-polarized light provides information only about species in solution within the gap between the electrode and the window[43] because the break down of symmetry selection rules producing measurable intensity occurs at about $\nu/4$. The p-polarized light bears all of the surface information as well as information about species in solution.[44]

A series of spectra obtained with s- and p-polarized light are displayed as conventional [45] $\Delta R/R$ versus ν plots, where ΔR is the difference between the intensity of the reflective signal at the sample and reference potentials, respectively. The reference intensity (R) was collected at $E_R = -0.2$ V, and sampling potentials covered the range $-1.2 < E/\text{V} < -0.6$. Downward bands correspond to substances produced either in the thin-layer solution or on the electrode surface. Upward bands reflect the disappearance of substances initially present.

The spectra obtained with p-polarized light (Figure 5b) show four interesting wavenumber regions characterized by a weak, negative band at 1674 cm^{-1}, a positive band at 1631 cm^{-1}, a negative band at 1519 cm^{-1}, and a band at ∼1390 cm^{-1} resembling a bipolar band. Similar bands are also observed with s-polarized light (Figure 5c).

The weak, negative band at 1674 cm^{-1}, which shows a decrease in intensity as *E* is shifted negatively, can be attributed to the asymmetric stretching of the N−C−N bonds in adsorbed perdeuterated FDS.[46] However, the intensity of the band at 1631 cm^{-1}, which is assigned to the disappearance of perdeuterated FDS from the solution,[46] increases as *E* is stepped from −0.6 to −0.8 V. The intensity of the negative band at 1519 cm^{-1}, which decreases as *E* is shifted negatively, has been assigned by Yan et al[46] to perdeuterated TU.

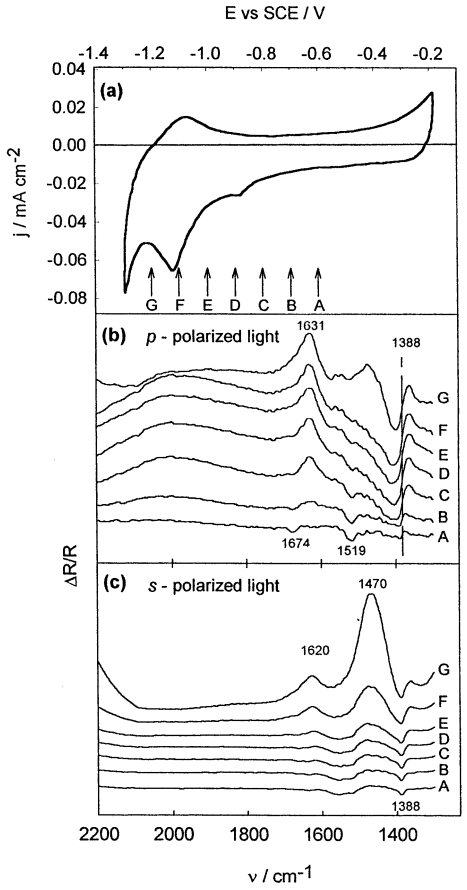

Figure 5. (a) Voltammogram of Ag(111) in perdeuterated 50 μM TU + 0.1 M $NaClO_4$ electrolyte run at 0.05 V sec^{-1}, 300 K. Labels A−G indicate potentials in $\Delta E = -0.1$ V steps ranging from $E = -0.6$ (A) to −1.2 V (G), where FT-IRRAS was performed. (b) s-polarized and (c) p-polarized FT-IRRAS differential spectra of polycrystalline silver. The reference spectrum was set at −0.2 V. Straight lines at $\nu = 1388$ cm^{-1} are drawn as visual guides.

The interpretation of the bipolar band at ~1390 cm^{-1} is rather complex because it can be attributed to either perdeuterated TU or FDS.[43,46] The negative lobe of this band increases in intensity (Figure 6a) as E is shifted negatively, reaching a maximum at $E = -1.1$ V. This fact is associated with the shift of ν from 1388 to 1402−1410 cm^{-1}. The intensity of the positive lobe of this bipolar band increases as E is shifted from −0.6 to −1.2 V, but its wavenumber remains constant at $\nu = 1360$ cm^{-1}. This suggests that this band results from the convolution of a positive band corresponding to the disappearance of a species that is present at E_R and absorbs at $\nu = 1360$ cm^{-1} and a negative band related to the appearance of a new species that absorbs at a slightly higher wavenumber. The negative band at 1388 cm^{-1} in s-polarized-light spectra (Figure 5c) is associated with the asymmetric stretching of the N−C−N bonds because it has been assigned to soluble perdeuterated TU.[46] However, the wavenumber of the broad negative band in the p-polarized-light spectra that lies in the range $1388 \leq \nu/cm^{-1} \leq 1410$, depending on E, can be related only to the presence of perdeuterated TU adsorbed on silver. An increase in the C−N bond order would serve to shift the C−N vibrational frequency of TU to higher values of ν. In fact, TU adsorption via the sulfur atom can produce such an increase in the C−N bond order. Therefore, the gradual increase in ν of the broad negative band suggests that the adsorbate ordering increases as E is shifted negatively and is complete at $E \approx -1.0$ V. The intensity of this band remains close to its maximum value in the range $-1.2 \leq E/V \leq -0.9$ and decreases slightly at $E = -1.2$ V.

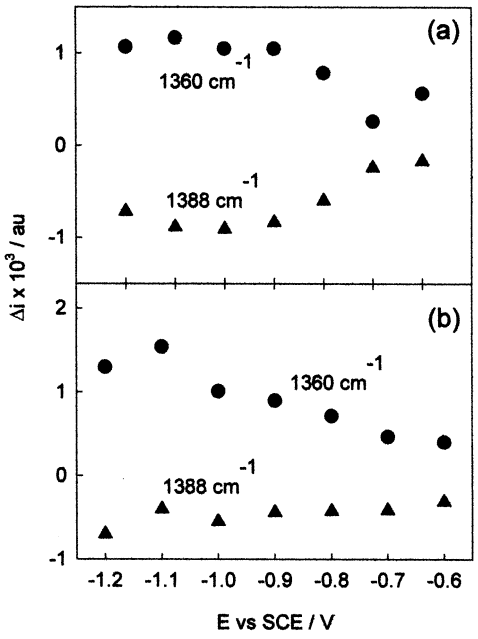

Figure 6. Relative intensity of the bipolar band at ca. 1390 cm^{-1} as a function of E, the applied potential. (a) s-polarized light. (b) p-polarized light.

The positive band at 1360 cm^{-1} cannot be straightforwardly assigned to any reactant or product. Its wavenumber lies close to 1399 cm^{-1}, the asymmetric stretching of the N−C−N bonds from perdeuterated FDS. This band could be shifted to 1360 cm^{-1} if it results from the convolution with the negative band at 1388 cm^{-1} related to TU. In fact, at the reference potential ($E_R = -0.2$ V), FDS is certainly produced electrochemically, as concluded from Figure 1. Accordingly, as E is stepped negatively, in both p- and s-polarized-light spectra (Figure 6a,b), the increase in the intensity of upward bands might be caused by the disappearance of the FDS signal at $E < E_R$ as compared to that collected at E_R. Concurrently, the decrease in TU electrooxidation as E is shifted negatively from −0.6 to −1.2 V produces an increase in the intensity of the negative band at 1388 cm^{-1} in p-polarized spectra. This increase can then be attributed to a change in the silver surface coverage by TU. This conclusion is consistent with the fact that no significant change is observed at 1388 cm^{-1} in spectra collected with s-polarized light.

To summarize, the presence of the negative band at 1388 cm^{-1}, recorded under conditions resulting in the same voltammetric features as those obtained from the ordered $d = 0.38$ and 0.44-nm hexagonal arrays on Ag(111), uniquely identifies the presence of adsorbed TU on polycrystalline silver. In addition, FT-IRRAS bands at 1674, 1631, and 1360 cm^{-1} confirm that FDS is a TU electrooxidation product on the polycrystalline substrate. The similar voltammetric responses of polycrystalline Ag and Ag(111) allow us to extend this conclusion to the Ag(111) surface.

The collection of voltammetric, STM, and FT-IRRAS data strongly point to self-assemblies of TU on Ag(111) in a $(\sqrt{7} \times \sqrt{7})R$ 19.1°−3X lattice, as is observed for alkanethiolates.[31−34] It is therefore tempting to assign the TU adsorbate to thioureate. Nevertheless, with these techniques, one cannot directly determine the chemical nature of sulfur in the TU adlayer. Consequently, XPS analyses of Ag(111)−TU samples were performed, as described below.

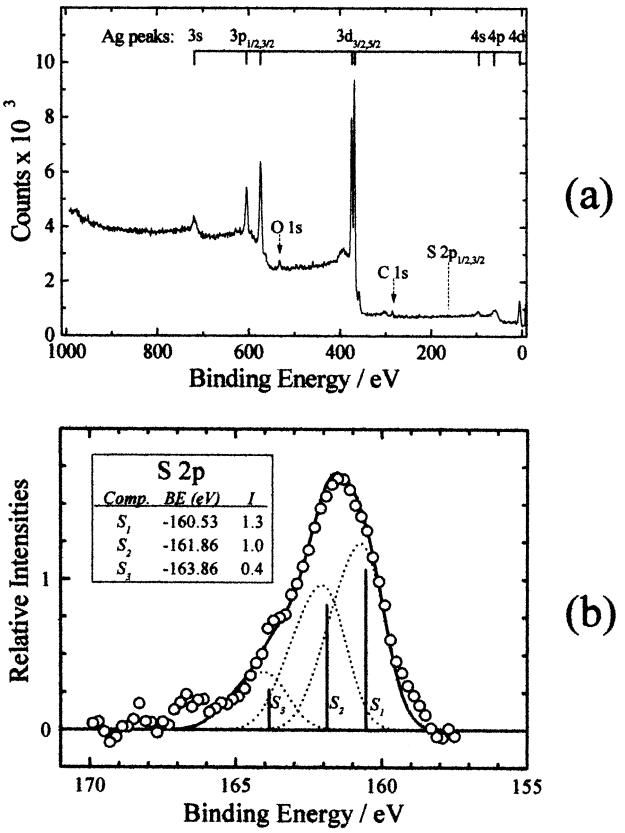

Figure 7. XPS spectra of Ag(111) after dipping for 10 s in aqueous 50 μM TU at *ocp*. (a) Broad (two scans) spectrum. (b) S 2p (2000 scans) spectrum. Dotted traces correspond to the deconvoluted spectrum.

3.4. Analyses of XPS Spectra. XPS spectra were obtained from Ag(111) samples that were dipped for 10 s into aqueous 50 μM TU and transferred in air into the XPS vacuum chamber. TU electrodesorption voltammograms of these samples[18] showed only the electrodesorption peak CII (Figure 1a), with a smaller charge (resulting in $\theta = 0.2$) due to the shorter time allowed for adsorption. Longer dipping[18] resulted in the peak multiplicity shown in Figure 1b. Ex situ STM images of these samples reveal regions with ordered Ag(111)$-(\sqrt{7} \times \sqrt{7})-$TU $d = 0.38$ nm and, less frequently, $d = 0.44$-nm hexagonal arrays.[18] Therefore, to determine the nature of the S$-$Ag bond in adsorbed TU, it is reasonable to perform XPS on samples prepared at *ocp*.

Survey and S 2p XPS spectra are displayed in Figure 7a and b, respectively. The survey spectrum (Figure 7a) is dominated by the Ag core-level peaks. O and C 1s peaks are also clearly visible. The structure at 400 eV, also reported for dodecanethiol$-$silver layered compounds[47] and either carbon- or oxygen-contaminated silver,[48] is too broad (20 eV) to be associated with a photoemission peak. Unfortunately, it completely masks any possible contribution from N. Many more scans are needed to reveal the presence of S (Figure 7b).

On the basis of measured peak intensities, tabulated photoemission cross sections, and electron mean free paths, we have estimated that the oxygen and carbon concentrations are near 1 ML each, whereas sulfur covers only about 0.1 ML. Sulfur coverage compares well with the $\theta = 0.2$-ML value estimated from electrodesorptive voltammetry.[18] Oxygen and carbon contamination levels are acceptable for an initially mostly uncovered surface that is as reactive as silver.

The cumulative 30 h S 2p photoelectron spectrum (Figure 7b) shows a broad peak centered at BE = 161.5 eV, with pronounced asymmetry toward larger binding energies and a clearly seen shoulder at 163.5 eV. Within noise limits, the main peak position and shape of the sequential S 2p spectra are found to be invariant over time, with at most a minimal (<5%) increase in possible sulfur-related oxides in the 166.0$-$169.6-eV BE region. The solid line in the Figure is the best fit to the cumulative spectrum with three Gaussian pairs. Different sulfur species associated with this fit at S $2p_{3/2}$ BE = 160.5 $\pm$ 0.2, 161.9 $\pm$ 0.1, and 163.9 $\pm$ 0.3 eV are labeled S_1, S_2, and S_3, respectively. Error bars indicate energy spans that produce good fits to data (<0.5% variation in rms) and should be compounded with the $\pm$0.3-eV instrumental error. Error in the minority species S_3 energy assignment decreases significantly at the high BE side by including small (<5%) sulfur oxide contributions in the 166.0$-$169.6-eV BE region[49] (not shown), while leaving main sulfur peak energy assignments essentially the same. Whereas as many as four sulfur species within a 3-eV BE range have been identified by high-resolution XPS for methylthiolate adsorption on Ni(111)[13] and Cu(111),[14] the quality of our data does not warrant such refinement.

TABLE 2: Characteristic S $2p_{3/2}$ Binding Energies (BE) for Sulfur and Sulfur-Containing Molecules That Are Free-Standing and Adsorbed on Transition Metals

S species	S moiety	S $2p_{3/2}$ BE (eV)	refs
sulfur	S adsorbed on Ag, Au	160.8$-$161.2	12, 47, 50$-$52
	S adsorbed on 3- and 4-fold Ni sites	161.15, 161.55, 162.10	53, 61
	S_n adsorbed on Ag, Au, Ni	162.0$-$162.3	39, 52, 54
	elemental S, S multilayer	163.0$-$164.5	47, 49[b],52
thiol (HSR[a])	adsorbed on Ag, Au	161.8$-$162.3	13, 11, 24, 47, 51, 55$-$57[b]
	adsorbed on Au defect sites	162.1, 162.4	24
	adsorbed on Ni sites	162.1$-$162.5, 163.3	60$-$61
	unbound thiol, dithiol	163.1$-$163.6	11, 49[b], 55, 63
thione	mesomeric ($-$S$-$C$\leq$)	161.3$-$161.8	49[b]
	normal (S$=$C$<$)	163.0$-$163.5	49[b]

[a] R = hydrocarbon chain. [b] Values of single peak maxima assigned to S 2p BE were converted to S $2p_{3/2}$ by subtraction of 0.4 eV.

The S 2p BEs of sulfur are characteristic of the molecular structure and are predominantly determined by the electronegativities of nearest-neighbor atoms. The BE for sulfur in certain structural elements can be predicted within narrow limits ($\pm$ 0.5 eV), as exquisitely presented by Lindberg et al. in a thorough and detailed review article.[49] These ranges, for individual structural elements, are small compared with the total range of BE. By comparing the BE of the components with previously published S 2p reference peaks, an assignment to different adsorbed sulfur species can be made. Table 2 gives a summary of some of the data published for sulfur and sulfur-containing molecules that are free-standing and adsorbed on silver, gold, and nickel. It shows that the minority sulfur species S_3 has various possible assignments including a neutral valence state. Those species labeled as S_1 and S_2 have lower BE values than S_3, suggesting that S is chemically bound to silver surface atoms. Therefore, these two components, besides jointly encompassing 85% of the adsorbed sulfur species (Figure 7b), are mainly

responsible for the charge transfer obtained in voltammetric experiments.

The assignment of the lowest BE component comes straight from Table 2. S_1 at 160.5 eV has the lowest binding energy, and its absolute value agrees, within the experimental resolution, with the BE values found for silver sulfide powder[47] and silver sulfide formed upon adsorption of sulfur[50] and hydrogen sulfide from the gas phase[12] on silver. Similar values are also reported for S adsorbed on Au(111),[51,52] whereas the high reactivity of nickel, as a result of the partially filled outer d shell, results in a 1-eV BE span for S adsorption on different Ni(111) sites.[53]

Species S_2, at 161.9 eV, has a concentration comparable to that of silver sulfide. From FT-IRRAS spectra, it was concluded that the electrodesorptive peak at $E \cong -1.2$ V corresponds to adsorbed TU. Therefore, we looked for TU species in this BE range and found the tautomeric forms of thiocarbonyls with broken S−H bonds.[49] In extending the comparison to other S-containing molecules, it should be noted that adsorbed thiolates have BE in the same energy window,[11,47,50,51,54−57] a single S 2p peak doublet is observed on Ag(111)[50] despite their well-established hollow−hollow-top self-assemblies, and thiolate adsorption on Au(111) defect sites results in BE decreases of less than 0.4 eV.[24] These are again indications of the similarities encountered for thiol and thiourea adsorbates on metals; besides similar voltammetric responses and adsorbed molecular assemblies, they have their BEs in the same energy window. Accordingly, the sulfur headgroup of TU on these substrates must largely resemble that found in thiolates (i.e., TU adsorbs as thioureate, the canonical form of TU with a cleaved S−H bond).

Whereas polymeric sulfur species on gold also have BE values in this range,[50,54] the concurrent absence of their characteristic STM images (trimers on Ag(111)[15]) and the presence of a N−C−N FT-IRRAS stretching mode suggest that, if present, polymeric sulfur is only a minority species.

The similar contributions of sulfide and thioureate to these ex situ XPS measurements is perhaps related to the strong adsorption of the doubly charged minority bisulfide species[58] that cleaves upon adsorption. Once nucleation of silver sulfide occurs, the sulfide islands grow laterally across the silver surface, limited by the supply of sulfur-containing species,[12] especially in cases where TU is not allowed to adsorb for a time sufficiently large so as to completely cover the electrode. Whereas main STM imaging and desorptive voltammetry are almost the same for TU adsorption both at *ocp* and under potentiostatic in situ experiments, the extent of ordered adsorbate regions and the voltammetric cathodic charge density values, q_c, are greater for the latter situation. In fact, recent in situ radiochemical experiments[59] have determined the presence of perpendicularly adsorbed TU with a surface concentration that is consistent with the value of q_c that we have observed for in situ experiments. The presence of ordered $d = 0.38$-nm hexagonal arrays and a single electrodesorptive peak in region I, under both in situ and ex situ conditions, leads us to conclude that the cumulative S 2p spectrum is highly representative of our system and therefore indicates that TU preponderantly adsorbs as thioureate.

By analogy with BE values reported for sulfur and sulfur-containing molecules that are free-standing and adsorbed on metals, the weaker component S_3 has many possible assignments (i.e., sulfur adsorbed either as multilayers or elemental sulfur,[50,54] FDS, unbound TU, and TU multilayers). Unfortunately, given the relatively small intensity of this component, neither an accurate peak position nor the actual number of species conforming to this component can be well defined from our experiments.

We purposely disregard possible contributions to component S_3 from site-dependent thioureate given that (i) silver has a full 4d shell and (ii) there are no measurable S 2p BE shifts reported for S and alkanethiol adsorbates on Ag(111).[50] This is in contrast to sulfur and methanethiol adsorption on Ni single crystals, where site-dependent differences in S 2p BE as large as ∼0.5 eV for a given Ni surface structure and ∼1 eV overall have been measured[60,61] as a result of the partially filled Ni 3d shell.

The lack of evidence of FDS arrays in ex situ STM images, the high reactivity of silver surfaces, and the facile cleavage the S−S bond upon adsorption of other disulfide-containing molecules at room temperature[59,61−64] also allow us to discard the possible presence of a measurable amount of FDS in direct contact with the Ag(111) surface. In the same sense, the presence of unbound isolated TU is also very improbable given the thorough rinsing with water after TU adsorption.[63]

In summary, TU adsorption on Ag(111) at *ocp* results in comparable amounts of silver sulfide and thioureate coexisting with one or more sulfur- or TU-derived minority compounds. Oxide formation, if any, is the result of sample degradation during the extended measurement period required by the weak S 2p signal, possibly accelerated by incident X-rays,[11] but this does not affect our main interpretation.

4. Conclusions

In situ and ex situ STM, FT-IRRAS, and XPS observations of Ag(111) and polycrystalline silver immersed in aqueous 50 μM TU solutions are presented.

Voltammetric and FT-IRRAS data show that the electroadsorption and electrodesorption processes of TU on silver are characterized by a pair of voltammetric peaks located at $E = -1.17$ and -1.23 V, respectively.

From voltammetric data, assuming a single electron-transfer process, an average degree of TU surface coverage of $\theta = 0.52$ ML is determined.

In situ STM images obtained just positive of anodic peak AII show three ordered hexagonal structures with $d = 0.44$ ($\theta = 0.43$), 0.38 ($\theta = 0.57$), and 0.33 nm ($\theta = 0.75$), depending on the applied potential and adsorption time.

Combined electrochemical and STM data suggest a rather slow, potential-dependent rate of the Ag(111) surface-coverage process by TU. It takes several minutes to reach quasi-equilibrium coverage. The three different adsorbate-induced hexagonal surface structures coexist spatiotemporally.

The voltammetric peak multiplicity (CII, CII′) observed in potential region II can be associated with a slow transformation between the different adsorbate-induced hexagonal surface structures and multilayer formation.

The positive shift in the asymmetric N−C−N stretching FT-IRRAS band at 1388 cm^{-1}, in potential region II, is associated with TU adsorption. FT-IRRAS spectra also confirm that, at more positive potentials, TU is electrooxidized to FDS.

XPS analyses of Ag(111) electrodes immersed in TU reveal comparable amounts of silver sulfide and thioureate coexisting with one or more sulfur- or TU-derived minority compounds.

Acknowledgment. The financial support of Agencia Nacional de Promoción Científica y Tecnológica (Argentina) PICT 99-5030 and CONICET (Argentina) PIP 0897-98 and PIP 4376-96 is gratefully acknowledged. V.B. and J.E.G. thank CONICET for fellowships. P.L.S. thanks AECI (Spain) for a fellowship.

We also thank G. Andreasen (INIFTA) and A. Trigubó (CITEFA) for their help with sample preparation.

References and Notes

(1) Ulman, A. *Chem. Rev.* **1996**, *96*, 1533.
(2) Ulman, A. *An Introduction to Ultrathin Organic Films from Langmuir−Blodgett to Self-Assembly*; Academic Press: San Diego, CA, 1991.
(3) Okinaka, Y.; Kato, M. *Modern Electroplating;* Schlesinger, M., Paunovic, M., Eds.; The Electrochemical Series, 4th ed.; Wiley & Sons: New York, 2000; pp 719−720.
(4) Bunge, E.; Port, S. N.; Roelfs, B.; Meyer, H.; Baumgärtel, H.; Schiffrin, D. J.; Nichols, R. J. *Langmuir* **1997**, *13*, 85.
(5) Azzaroni, O.; Andreasen, G.; Blum, B.; Salvarezza, R. C.; Arvia, A. J. *J. Phys. Chem. B* **2000**, *104*, 1395.
(6) Bunge, E.; Nichols, R. J.; Roelfs, B.; Meyer, H.; Baumgärtel, H. *Langmuir* **1996**, *12*, 3060.
(7) Mayer, R. In *Organosulfur Chemistry;* Janssen, M., Ed.; Interscience: New York, 1967; p 219.
(8) Fleishmann, M.; Hill, I. R.; Sundholm, G. *J. Electroanal. Chem.* **1983**, *157*, 359.
(9) Rodriguez, J. A.; Hrbek, J. *Acc. Chem. Res.* **1999**, *32*, 719.
(10) Bryant, M. A.; Pemberton, J. E. *J. Am. Chem. Soc.* **1991**, *113*, 8284.
(11) Laibinis, P. E.; Whitesides, G. M.; Allara, D. L.; Tao, Y. T.; Parikh A. N.; Nuzzo, R. G. *J. Am. Chem. Soc.* **1991**, *113*, 7152.
(12) Graedel, T. E.; Franey, J. P.; Gaultieri, G. J.; Kammlott, K. W.; Malm, D. L. *Corros. Sci.* **1985**, *25*, 1163.
(13) Rufael, T. S.; Huntley, D. R.; Mullins D. R.; Gland, J. L. *J. Phys. Chem* **1995**, *99*, 11472.
(14) Jackson, G. J.; Woodruff, D. P.; Jones, R. G.; Singh, N. K.; Chan, A. S. Y.; Cowie B. C. C.; Formoso, V. *Phys. Rev. Lett.* **2000**, *84*, 119.
(15) Aliosi, G. D.; Cavallini, M.; Innocenti, M.; Foresti, M. L.; Pezzatini, G.; Guidelli, R. *J. Phys. Chem B* **1997**, *101*, 4774.
(16) Hatchett, D. W.; Gao, X.; Catron, S. W.; White, H. S. *J. Phys. Chem.* **1996**, *100*, 331.
(17) Hatchett D. W.; White, H. S. *J. Phys. Chem.* **1996**, *100*, 9854.
(18) Brunetti, V.; Blum, B.; Salvarezza, R. C.; Arvia, A. J. *Acta Microscopica* **2001**, *10 (suppl. 1)*, 147.
(19) Hatchett, D. W.; Stevenson, K. J.; Lacy, W. B.; Harris, J. M.; White, H. S. *J. Am. Chem. Soc.* **1997**, *119*, 6596.
(20) Hatchett, D. W.; Uibel, R. H.; Stevenson, K. J.; Harris, J. M.; White, H. S. *J. Am. Chem. Soc.* **1998**, *120*, 1062.
(21) Mohtat, N.; Byloos, M.; Soucy, M.; Morin, S.; Morin, M. *J. Electroanal. Chem.* **2000**, *484*, 120.
(22) Widrig, C. A.; Chung, C.; Porter, M. D. *J. Electroanal. Chem.* **1991**, *310*, 335.
(23) Yang, D.-F.; Wilde, C. P.; Morin, M. *Langmuir* **1997**, *13*, 243.
(24) Walczak, M. M.; Alves, C. A.; Lamp, B. D.; Porter, M. D.; *J. Electroanal. Chem.* **1995,** *396*, 103.
(25) Andreasen, G.; Vericat, C.; Vela, M. E.; Salvarezza, R. C. *J. Chem. Phys.* **1999**, *111*, 9457.
(26) Vericat, C.; Andreasen, G.; Vela, M. E.; Salvarezza, R. C. *J. Phys. Chem.* **2000**, *104*, 302.
(27) Zhong, C.-J.; Porter, M. D. *J. Electroanal. Chem.* **1997,** *425*, 147.
(28) Wong, S.-S.; Porter, M. D. *J. Electroanal. Chem.* **2000,** *485*, 135.
(29) Schwaha, K.; Spencer, N. D.; Lambert, R. M. *Surf. Sci.* **1979**, *81*, 273.
(30) Sellers, H.; Ulman, A.; Shnidman, Y.; Eilers, J. E. *J. Am. Chem. Soc.* **1993**, *115*, 9389.
(31) Heinz, R.; Rabe, J. P. *Langmuir* **1995**, *11*, 506.
(32) Fenter, P.; Eisenberger, P.; Li, J.; Camillone, N., III; Bernasek, S.; Scoles, G.; Ramanarayanan, T. A.; Liang, K. S. *Langmuir* **1991**, *7*, 2013.
(33) Dhirani, A.; Hines, M. A.; Fisher, A. J.; Ismail, O.; Guyot-Sionnest, P. *Langmuir* **1995**, *11*, 2609.
(34) Rieley, H.; Kendall, G. K.; Jones, R. G.; Woodruff, D. P. *Langmuir* **1999**, *15*, 8856.
(35) Dubois, L. H.; Zegarski, B. R.; Nuzzo, R. G. *J. Chem. Phys.* **1993**, *98*, 3503.
(36) Moulder, J. F.; Stickle, W. F.; Sobol, P. E.; Bomben, K. D. In *Handbook of X-ray Photoelectron Spectroscopy: A Reference Book of Standard Spectra for Identification and Interpretation of XPS Data*; Chastain, J., Ed.; Perkin-Elmer Corporation: Eden Prairie, MN, 1992.
(37) Hecht, D.; Strehblow, H.-H. *J. Electroanal. Chem.* **1997**, *440*, 211.
(38) Jennings, G. K.; Laibinis, P. E. *J. Am. Chem. Soc.* **1997**, *119*, 5208.
(39) Salaneck, W. R.; Lipari, N. O.; Paton, A.; Zallen, R.;. Liang, K. S. *Phys. Rev. B* **1975**, *12*, 1493.
(40) Foresti, M. L.; Innocenti, M.; Forni, F.; Guidelli, R. *Langmuir* **1998**, *14*, 7008.
(41) Gupta, P. C. *Z. Anal. Chem.* **1963**, *196*, 412.
(42) Bolzan, A. E.; Piatti, R. C. V.; Salvarezza, R. C.; Arvia, A. J. *J. Appl. Electrochem.*, submitted for publication.
(43) Papapanayiotou, D.; Nuzzo, R. N.; Alkire, R. C. *J. Electrochem. Soc.* **1998**, *145*, 3366.
(44) Corrigan, D. S.; Weaver, J. J. *J. Electroanal. Chem.* **1988**, *239*, 55.
(45) Beden, B.; Lamy, C. In *Spectroelectrochemistry: Theory and Practice;* Gale, R. J., Ed.; Plenum Press: New York, 1988; p 189.
(46) Yang, M.; Liu, K.; Jiang, Z. *J. Electroanal Chem*. **1996,** *408*, 225 and references therein.
(47) Bensebaa, F.; Zhou, Y.; Deslandes, Y.; Kruus, E.; Ellis, T. H. *Surf. Sci.* **1998**, *405*, L472.
(48) Obretenov, W.; Höpfner, M.; Lorenz, W. J.; Budevski, E.; Staikov, G.; Siegenthaler, H. *Surf. Sci.* **1992**, *271*, 191.
(49) Lindberg, B. J.; Hamrin, K.; Johansson, G.; Gelius, U.; Fahman, A.; Nordling, C.; Siegbahn, K. *Phys. Scr.* **1970**, *1*, 286.
(50) Zemek, J.; Jiricek, P.; Hucek, S.; Jablonski, A.; Lesiak, B. *Surf. Sci.* **2001**, *473*, 8.
(51) Weishaar, D. W.; Walczak, M. M.; Porter, M. D. *Langmuir* **1993**, *9*, 323.
(52) Vericat, C.; Vela, M. E.; Andreasen, G.; Salvarezza, R. C. *Langmuir* **2001**, *17*, 4919.
(53) Mullins, D. R.; Huntley, D. R.; Overbury, S. H. *Surf. Sci.* **1995**, *323*, L287.
(54) Buckley, A. N.; Hamilton, I. C.; Woods, R. *J. Electroanal. Chem.* **1987**, *216*, 213.
(55) Zubrägel, Ch.; Deuper, C.; Schneider, F.; Neumann, M.; Grunze, M.; Schertel, A.; Wöll, Ch. *Chem. Phys. Lett.* **1995**, *238*, 308.
(56) Frey, S.; Heister, K.; Zharnikov, M.; Grunze, M.; Tamada, K.; Colorado, R., Jr.; Graupe, M.; Scmakova, O. E.; Lee, T. R. *Isr. J. Chem.* **2000**, *40*, 81.
(57) Tarlov, M. J.; Burgess, D. R. F., Jr.; Gillen, G. *J. Am. Chem. Soc.* **1993**, *115*, 5305.
(58) Tao, Y. T.; Panchan, K.; Lee, W. Ch. *J. Am. Chem. Soc*. **2000**, *122*, 7072.
(59) Sobkowski, J.; Smolinski, S. *Abstracts*, no. 1027, 2001 Joint International Meeting of The Electrochemical Society and The International Society of Electrochemistry, San Francisco, CA, 2001.
(60) Mullins, D. R.; Huntley, D. R.; Tang, T.; Saldin, D. K.; Tysoe, W. T.; *Surf. Sci.* **1997**, *380*, 468.
(61) Rufael, T. S.; Huntley, D. R.; Mullins, D. R.; Gland, J. L. *J. Phys. Chem. B* **1998**, *102*, 3431.
(62) Nuzzo, R. G.; Zegarski, B. R.; Dubois, L. H. *J. Am. Chem. Soc.* **1987**, *109*, 733.
(63) Castner, D. G.; Hinds, K.; Grainger, D. W. *Langmuir* **1996**, *12*, 5083.
(64) Ishida, T.; Yamamoto, S.; Mizutani, W.; Motomatsu, M.; Tokumoto, H.; Hokari, H.; Azehara, H.; Fujihira, M. *Langmuir* **1997**, *13*, 3261.